

Additional Insights into Luminescence Process of Polycyclic Aromatic Hydrocarbons with Carbonyl Groups: Photophysical Properties of Secondary *N*-Alkyl and Tertiary *N,N*-Dialkyl Carboxamides of Naphthalene, Anthracene, and Pyrene

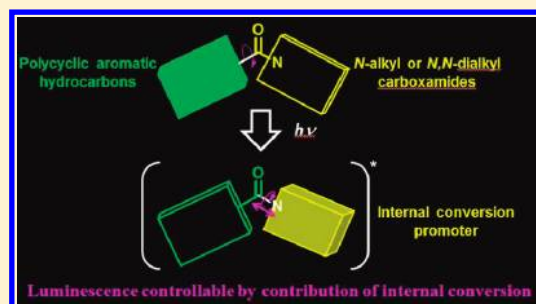
Yosuke Niko,[†] Yuki Hiroshige,[†] Susumu Kawauchi,[†] and Gen-ichi Konishi^{*,†,‡}

[†]Department of Organic and Polymeric Materials, Tokyo Institute of Technology, O-okayama, Tokyo 152-8552, Japan

[‡]PRESTO, Japan Science and Technology Agency (JST), Kawaguchi, Saitama 332-0012, Japan

S Supporting Information

ABSTRACT: Here we report the substitution effects of *N*-alkyl and *N,N*-dialkyl carboxamide groups on the fluorescence properties of polycyclic aromatic hydrocarbon chromophores, so as to control their fluorescence properties. The fluorescence properties of compounds obtained using solvents with different polarities showed very little change, indicating that the modified compounds do not form charge transfer states. TD-DFT calculations and measurements performed at low temperature (78 K) and in viscous solvents revealed that the *N*-alkyl and *N,N*-dialkyl carboxamide groups tend to reduce the contributions from intersystem crossing and increase those from internal conversion. Considering that the fluorescence mechanism of low-fluorescence carbonyl compounds such as aldehyde and ketone is dominated by intersystem crossing and that of high-luminescence carbonyl compounds such as carboxylic acid and ester is dominated by a radiative process, it can be said that the photophysical process of *N*-alkyl and *N,N*-dialkyl carboxamides is novel. In addition, the calculation results for excited states indicated that such contributions can be controlled by selecting the appropriate polycyclic aromatic hydrocarbon or amide structure, in addition to solvent viscosity and temperature.



INTRODUCTION

For decades, organic emission dyes have attracted considerable attention owing to their potential application as molecular electronic materials in organic electroluminescent and photoluminescent devices, as well as their use in organic field effect transistors, liquid crystal laser dyes, and fluorescence probes and sensors. A large number of organic dyes based on luminescent polycyclic aromatic hydrocarbon structures such as naphthalene,¹ anthracene,^{2–6} pyrene,^{7–19} fluorene,^{20–25} and perylene^{26–28} have been developed. Organic dye molecules have specifically been designed for many purposes, including the enhancement of emission efficiency, control of emission color, and improvement of solubility in organic solvents or other matrices. The general strategy for the development of novel dyes relies on the introduction of various substituents to the target molecule. In particular, enhancement of emission properties or control of emission color has been achieved through the expansion of π -conjugation induced by, e.g., phenyl or ethynyl groups,^{29–33} introduction of σ - π conjugation induced by silyl groups,^{34–37} and the use of charge transfer emission induced by highly polarized groups.^{38–45} These chromophores can be introduced into structures that are suitable for emissions, such as polymers in the main or side chain,^{46–50} spiro skeletons,^{51–55} and rod- or star-shaped chromophores.^{56–59} Thus, understanding the manner in which substituents affect chromophores and finding ways to

control their emission properties is extremely valuable for the molecular design of a wide variety of materials. As there are many potential substituents that have not yet been studied, there is a great deal of knowledge to be gained that may lead to the acquisition of a new design guide for new materials in this field.

Most carbonyl substituents have well-known characteristic effects on the emission properties of chromophores. The photophysical processes of chromophores modified by such substituents have been examined in detail. For instance, dyes directly bearing aldehyde or ketone groups fluoresce weakly because of intersystem crossing, as rationalized by the El-Sayed rule.^{60–66} In addition, luminophores such as benzamide modified by anilide groups exhibit low levels of luminescence because they form twisted intramolecular charge transfer (TICT) states.^{67–70} In contrast, chromophores possessing a carboxylic acid or its ester groups exhibit strong fluorescence.^{71–79} Many of these carbonyl compounds have already been used in environmentally responsive probes or sensitizers.^{70,74–76}

Although carbonyl compounds have been widely investigated, research on the synthesis and photoluminescence properties of *N*-alkyl or *N,N*-dialkyl aromatic carboxamide

Received: February 21, 2012

Published: March 29, 2012

compounds is surprisingly limited, except the studies by our group on the environmentally responsive emission^{83,84} or other groups on the use as fluorescence probes^{80–82} of pyrene-1-carboxamides and those by Sturgeon and Schulman group and Werner and Rodgers group on *N,N*-diethylantracene-9-carboxamide.^{85,86} None of these studies investigated the effects of *N*-alkyl or *N,N*-dialkyl carboxamide groups on chromophores in much detail, assessing only a small number of compounds or collecting only partial experimental data. The photophysical properties of most aromatic carbonyl compounds have been generally rationalized by intersystem crossing, internal conversion, and charge transfer. Our previous studies have indicated that the photophysical properties of *N*-alkyl and *N,N*-dialkyl carboxamides are strongly dependent on the contribution of internal conversion;⁸³ however, little was investigated in terms of the other two processes. Each of these processes has recently been recognized as considerably important because of their utility in electronic devices.^{87–89} Therefore, it is important to understand not only the fluorescence properties of a material but also the photophysical processes that can be induced by fundamental compounds such as *N*-alkyl and *N,N*-dialkyl carboxamides.

In this study, we demonstrated that polycyclic aromatic hydrocarbons with *N*-alkyl or *N,N*-dialkyl carboxamide groups show a new photophysical process where internal conversion is a more competitive process and which is apparently different from other carbonyl compounds as described in Figure 1. We

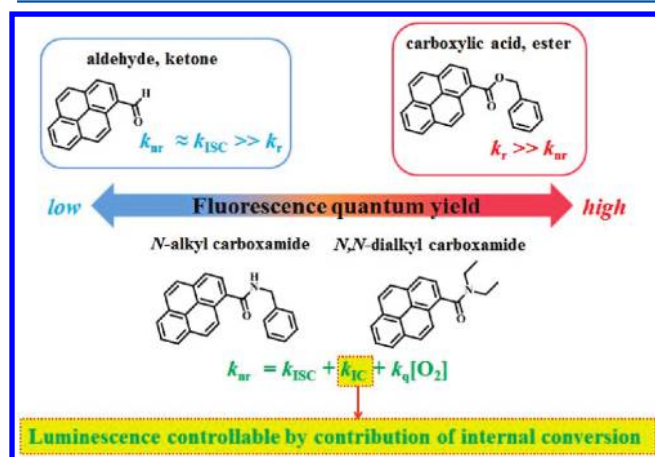


Figure 1. Relationships between fluorescence quantum yield and photophysical process in carbonyl compounds. k_r , k_{nr} : Rate constants for radiative and non-radiative process, respectively. k_{ISC} , k_{IC} , $k_q[O_2]$: Rate constants for intersystem crossing, internal conversion, quenching by oxygen, respectively.

synthesized several *N*-alkyl and *N,N*-dialkyl polycyclic aromatic carboxamides based on naphthalene, anthracene, and pyrene as target polycyclic aromatic hydrocarbon dyes. We then examined their photoluminescence properties in detail to understand how these substituent groups affect the photophysical properties of such chromophores. The main advantages of *N*-alkyl and *N,N*-dialkyl carboxamide groups are their convenient synthesis and flexibility in molecular design, which make them attractive candidates for controlling the fluorescence properties of dyes and their subsequent application to the production of functional materials. Naphthalene, anthracene, and pyrene are used for the evaluation of substituent effects, as they are very simple polycyclic aromatic hydrocarbons and their photophysical processes have been well characterized.^{90–93} Moreover, these polycyclic aromatic hydrocarbons, especially anthracene and pyrene, are easy to use because they have been employed widely in the development of emissive materials.

RESULTS AND DISCUSSION

Synthesis. Using a previously reported method,⁸³ we synthesized secondary *N*-alkyl and tertiary *N,N*-dialkyl carboxamide derivatives of naphthalene, anthracene, and pyrene, designated as **Nap 1**, **Nap 2**, **Anth 1**, **Anth 2**, **Py 1a**, and **Py 2a**, respectively. Naphthalene, anthracene, and pyrene were derivatized at the 2, 9, and 1 positions, respectively. Their chemical structures are shown in Figure 2. With respect to the pyrene derivatives, we have previously prepared several *N*-alkyl and *N,N*-dialkyl carboxamide (**Py 1b**, **1c** and **2a**, **2c**) and demonstrated that the fluorescence behavior of both *N*-alkyl type and *N,N*-dialkyl type pyrene-1-carboxamides did not depend significantly on changes in the structure of the alkyl chain in an ethanol solution.⁸³ Therefore, here we have focused on one derivative per chromophore for both the *N*-alkyl and *N,N*-dialkyl derivatives.

Structures and Photophysical Properties. The UV–vis spectra, fluorescence spectra, absolute fluorescence quantum yields, and fluorescence lifetimes of *N*-alkyl and *N,N*-dialkyl aromatic carboxamides were measured in deaerated ethanol. In addition, optimized structures were calculated by the density functional theory (DFT) method at the ω B97X-D/6-31G(d,p) level (Figure 1S, Supporting Information). These measurements were performed to examine the photoluminescence properties and compare the secondary *N*-alkyl carboxamides with the tertiary *N,N*-dialkyl carboxamides. Measurements were also carried out in other solvents in order to investigate the changes in the absorption and emission spectra caused by solvent polarization. The results are shown in Figure 2S, Figure 3S, and Table 1S (Supporting Information).

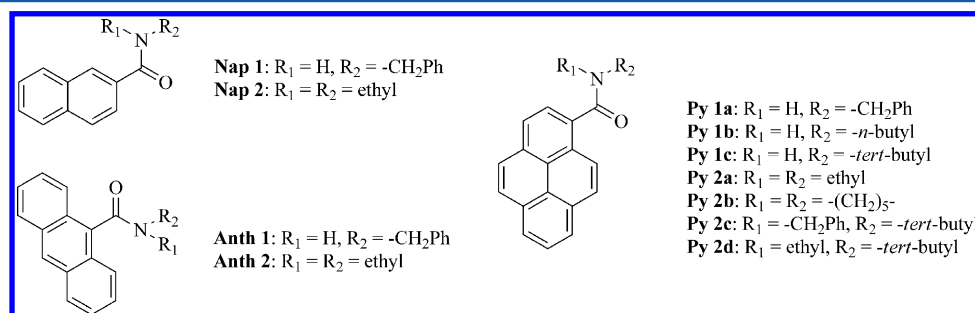


Figure 2. Chemical structures of *N*-alkyl and *N,N*-dialkyl aromatic carboxamides used in this study.

Naphthalene. As shown in Figure 3, no significant differences were observed between the UV–vis spectra for

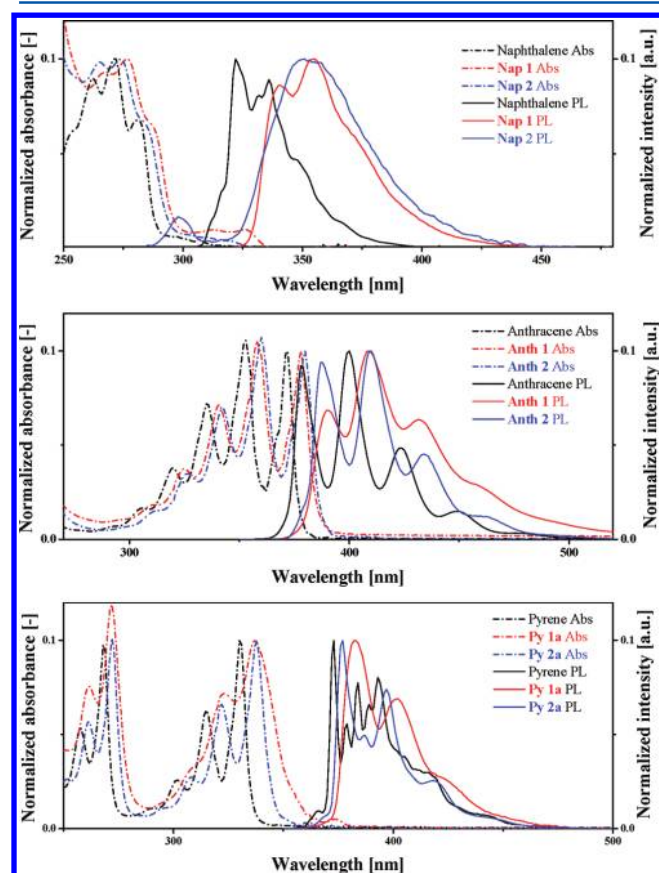


Figure 3. UV–vis and fluorescence spectra of *N*-alkyl and *N,N*-dialkyl carboxamides, measured in ethanol (room temperature, $\lambda_{\text{ex}} = \lambda_{\text{abs}}$).

Nap 1 and Nap 2. As compared to the spectra of unsubstituted naphthalene, those of substituted naphthalene were red-shifted and did not retain their clear vibrational structure. The fluorescence spectra and absolute fluorescence quantum yield measurements revealed that **Nap 1** showed a strong emission ($\Phi_{\text{fl}} = 0.28$) around 350 nm and exhibited a rather broad spectrum. In contrast, **Nap 2** exhibited extremely weak emission ($\Phi_{\text{fl}} < 0.01$) around 340 nm, with an intensity close to that of the ethanol Raman signal at around 300 nm. From the optimized ground-state structures calculated by the DFT method, **Nap 1** and **Nap 2** were found to form dihedral angles

of approximately 26.9° and 43.2° with respect to the naphthalene rings and carbonyl groups, respectively.

Anthracene. Similar to the naphthalene derivatives, no significant differences were observed between the absorption spectra for **Anth 1** and **Anth 2**. In addition, the spectra were red-shifted relative to unsubstituted anthracene. **Anth 1** and **Anth 2** showed fluorescence at similar wavelengths, but the vibrational structures were somewhat different. As seen in Table 1, **Anth 1** had a fluorescence quantum yield smaller than that of unsubstituted anthracene but larger than that of **Anth 2**. Similar to anthracene carboxylic acid and its ester derivatives, **Anth 1** and **Anth 2** showed large dihedral angles of approximately 64.4° and 82.9° with respect to the anthracene rings and carbonyl groups, respectively.

Pyrene. In our previous work, the absorption and fluorescence wavelengths of **Py 1a** and **Py 2a** were found to be similar and red-shifted and the vibrational structures were found to be same. Furthermore, in the fluorescence spectra of **Py 1a** and **Py 2a**, the well-known “Ham effect”,⁹⁰ i.e., the clear vibrational structure seen in the fluorescence spectrum of unsubstituted pyrene, was lost. **Py 1a** showed a fluorescence quantum yield higher than that of pyrene, whereas **Py 2a** exhibited a much weaker emission. Optimized structures of **Py 1a** and **Py 2a** were found to form dihedral angles of 45.4° and 76.8° with respect to the pyrene rings and carbonyl groups, respectively.

From these results, we note the following important trends:

- (1) Fluorescence quantum yields of *N*-alkyl carboxamides were higher than those of *N,N*-dialkyl carboxamides, especially for the naphthalene and pyrene derivatives.
- (2) The absorption and emission wavelengths of all the compounds were red-shifted. Simultaneously, the Stokes shifts of all of the compounds were slightly enlarged. These trends were observed when other solvents such as cyclohexane, dichloromethane, and acetonitrile were used (Figure 2S and Table 1S, Supporting Information). However, in almost all of the compounds, no clear relationships between the solvent polarities and Stokes shifts were observed. From the small slopes of all of the Lippert–Mataga plots in Supplementary Figure 3S, it was demonstrated that the changes in the dipole moments in the ground and excited states were small.⁹⁵ This means that these compounds did not accept the charge transfer states, e.g., via twisted intramolecular charge transfer (TICT).

Table 1. Photophysical Parameters of *N*-Alkyl and *N,N*-Dialkyl Carboxamides in Ethanol

entry	λ_{abs} [nm]	$\log \epsilon$ [$\text{M}^{-1} \text{cm}^{-1}$]	λ_{em} [nm]	τ [ns]	Φ_{fl}	k_{r}^a [s^{-1}]	k_{nr}^b [s^{-1}]
naphthalene	272	3.67	322, 332, 336	50.5 ⁹⁴	0.14	2.8×10^6	1.7×10^7
Nap 1	277	3.90	341, 354	9.19	0.28	3.0×10^7	7.8×10^7
Nap 2	274		351	0.51 (0.17) 1.58 (0.65) 6.70 (0.18)	0.003		
anthracene	372	3.89	378, 400, 423, 449	5.07 ⁹⁴	0.26	5.1×10^7	1.5×10^7
Anth 1	378	3.94	390, 409, 432	1.54	0.10	6.6×10^7	5.8×10^8
Anth 2	380	4.01	388, 410, 434, 462	1.15	0.062	5.4×10^7	8.2×10^8
pyrene	330	4.62	373, 379, 384, 389, 393	113 ⁹⁴	0.39	3.5×10^6	5.4×10^7
Py 1a	337	4.49	383, 402, 425	27.1	0.61	2.3×10^7	1.4×10^7
Py 2a	338	4.49	377, 387, 397, 419	30.4	0.061	2.0×10^6	3.1×10^7

^a k_{r} : radiative rate constant. $k_{\text{r}} = \Phi_{\text{fl}}/\tau$. ^b k_{nr} : non-radiative rate constant. $k_{\text{nr}} = (1 - \Phi_{\text{fl}})/\tau$.

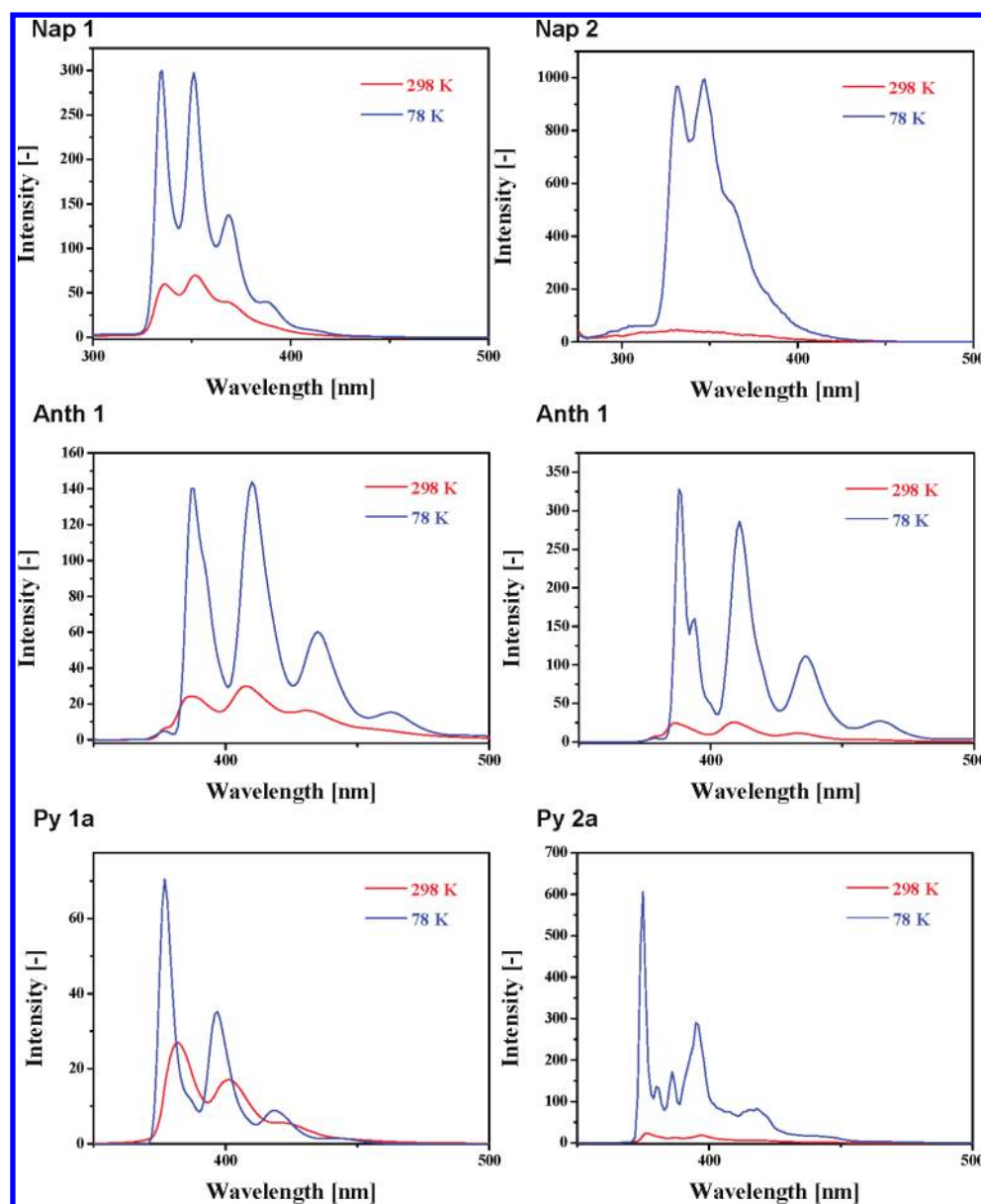


Figure 4. Fluorescence spectra of *N*-alkyl and *N,N*-dialkyl carboxamides at 298 and 78 K (EPA solvent, $\lambda_{\text{ex}} = \lambda_{\text{abs}}$).

- (3) In the ground states, both *N*-alkyl and *N,N*-dialkyl carboxamides formed large dihedral angles with respect to the aromatic rings and carbonyl groups, as generally observed for anilide type compounds^{96,97} or 9-substituted anthracene carbonyl compounds.^{61,62,73,77–79}

In general, the fluorescence emission properties of aromatic carbonyl compounds are explained by contributions from two deactivation processes. The first is the electronic factor for intersystem crossing, rationalized by the El-Sayed rule,^{64–66} and the second is the Franck–Condon factor for internal conversion.⁷⁶ It is known that the low fluorescence efficiencies of aldehyde and ketone derivatives are due to the former process.^{60–63} On the other hand, it is known that carboxylic acid and ester derivatives of naphthalene, anthracene, and pyrene are highly emissive. These compounds undergo intersystem crossing inefficiently and can prevent internal conversion owing to the planar rigid structures formed in the excited states.^{71–79} Such planar structures enable the formation of hydrogen bonds between the aromatic rings and the

carboxylic acid or ester groups and, as a result, form rigid structures. In addition, some compounds are quenched by another mechanism. For example, it is known that the low level of fluorescence of anilide-type compounds such as benzanilide is due to the formation of twisted intramolecular charge transfer (TICT) states with subsequent quenching by internal conversion.^{67–70} Thus, the following hypotheses can be proposed.

From trends 1 and 2, it is expected that the photophysical processes of the *N*-alkyl and *N,N*-dialkyl aromatic carboxamides are determined not by the charge transfer state as in benzanilide but by the contributions of both intersystem crossing and internal conversion, similar to aromatic aldehyde, ketone, and carboxylic acid and its ester derivatives. Furthermore, trend 3 suggests that if the deactivations are caused by internal conversion, the contribution of internal conversion depends strongly on the dihedral angle between the polycyclic aromatic rings and carbonyl groups in the ground and excited states.

Solvent Thermal and Viscosity Effect on Photophysical Properties. To investigate the photophysical processes of *N*-alkyl and *N,N*-dialkyl aromatic carboxamides in detail, the dependence of fluorescence on temperature and solvent viscosity were measured for **Nap 1**, **Nap 2**, **Anth 1**, **Anth 2**, **Py 1a**, and **Py 2a**. The thermal dependence was evaluated by measuring the fluorescence spectra and relative quantum yields at room temperature as well as at low temperatures (298 and 78 K) using the organic glass solvent EPA (a mixture of diethyl ether, isopentane, and ethanol). Furthermore, the relative fluorescence quantum yields were calculated using the absolute fluorescence quantum yield at 298 K as the standard. The solvent viscosity dependence was evaluated by measuring the fluorescence spectra, absolute quantum yields, and fluorescence lifetimes in ethanol, ethylene glycol, and glycerin solutions. These results are summarized in Table 2S and Figure 4S (Supporting Information).

As shown in Figure 4 and Table 2, the fluorescence intensities and quantum yields of almost all of the compounds

Table 2. Photophysical Parameters of Naphthalene, Anthracene, Pyrene, and Their *N*-Alkyl and *N,N*-Dialkyl Carboxamide Derivatives at 298 and 78 K

	<i>T</i> [K]	λ_{em} [nm]	Φ_f^c
naphthalene	298	322, 336, 348	0.023
	78	316, 321, 331, 336, 341, 347	0.22
Nap1	298	336, 352, 370	0.12
	78	334, 350, 368, 389	0.39
Nap2	298	330	0.007
	78	329, 344, 360	0.08
anthracene	298	377, 399, 422, 448	0.25
	78	380, 402, 426, 453	0.23
Anth 201	298	387, 407, 431	0.086
	78	388, 411, 436	0.28
Anth 216	298	387, 409, 433, 461	0.043
	78	388, 394, 411, 436, 465	0.34
pyrene	298	373, 379, 384, 393	0.16
	78	372, 378, 383, 393, 415	0.45
Py 1a	298	382, 401, 424	0.69
	78	376, 387, 396, 418	0.94
Py 2a	298	376, 387, 397, 419	0.054
	78	375, 380, 386, 395, 418	0.66

^c Φ_f : fluorescence quantum yields at 78 K were calculated using the value of absolute fluorescence quantum yield at room temperature (298 K) as the standard.

dramatically increased at low temperatures. Similarly, the fluorescence intensities and quantum yields were enhanced with an increase in the solvent viscosity. Additionally, the non-radiative rate constant k_{nr} decreased with an increase in the solvent viscosity. k_{nr} can be expressed as $k_{nr} = k_{ISC} + k_{IC} + k_q[O_2]$, where k_{ISC} , k_{IC} , and $k_q[O_2]$ denote the rate constants for intersystem crossing, internal conversion, and fluorescence quenching by oxygen, respectively. Considering that all the samples were deoxygenated, $k_q[O_2]$ was assumed to be almost zero. Furthermore, k_{IC} is assumed to be small at a low temperature or in viscous media.⁹⁸ Therefore, it is inferred that the above-mentioned phenomena were the result of the suppression of internal conversion.

However, it has been shown that the fluorescence intensity is enhanced when the intersystem crossing is reduced by the suppression of the activation energies between S_1 and the

triplet near S_1 .⁹⁹ Therefore, we also investigated the thermal dependence of naphthalene, anthracene, and pyrene (Figure 5S, Supporting Information). In the measurements for unsubstituted pyrene and naphthalene, increases in the fluorescence intensities were observed at 78 K. This occurred because the intersystem crossing was suppressed by the inefficient internal conversions from S_1 to S_0 generally observed for such rigid hydrocarbons.⁹⁰ On the other hand, the fluorescence intensity of unsubstituted anthracene remained almost constant. This was because, in the photophysical processes of anthracene, the contribution of internal conversion was originally small, as noted above, and the energy gap between S_1 and T_2 was too small to prevent intersystem crossing, as previously reported.^{93,100}

In the measurements for **Py 1a** and **Py 2a**, both compounds, especially **Py 1a**, showed high fluorescence levels at 78 K, which were stronger than those of unsubstituted pyrene. Given that the rate constants of the internal conversion were almost zero at 78 K, it is likely that **Py 1a** and **Py 2a** possess electronic structures with inefficient intersystem crossings relative to unsubstituted pyrene, leading to strong emission at 78 K. However, at room temperature, **Py 2a** had extremely low fluorescence, whereas **Py 1a** was highly emissive. It was hypothesized that this is because **Py 2a** underwent another competitive deactivation process, internal conversion, which was due to the *N,N*-dialkyl carboxamide group.

Similar to the pyrene derivatives, the anthracene derivatives, **Anth 1** and **Anth 2**, exhibited fluorescence levels stronger than those of unsubstituted anthracene at 78 K. We interpreted this to mean that the intersystem crossings of **Anth 1** and **Anth 2** were less efficient than those of anthracene. Furthermore, it can be said that the weak emissions of **Anth 1** and **Anth 2** compared to anthracene at room temperature were the result of internal conversion because of the new deactivation components supplied by the *N*-alkyl and *N,N*-dialkyl carboxamide groups.

In the investigation into the naphthalene derivatives, it was demonstrated that **Nap 1** showed similar behavior as **Py 1a**, possessing an electronic structure where the intersystem crossing was less efficient than for the unsubstituted naphthalene. Therefore **Nap 1** emitted more strongly at both 78 K and room temperature. In contrast, **Nap 2** had extremely low luminescence at both 78 K and room temperature. As discussed above, because the *N*-alkyl and *N,N*-dialkyl carboxamides may possess new competitive components of internal conversion, we think that, for **Nap 2**, the contributions of both the intersystem crossing and internal conversion were large.

TD-DFT Calculations. Electronic Structure and Singlet and Triplet Energies of *N*-Alkyl and *N,N*-Dialkyl Aromatic Carboxamides. In order to examine whether quenching by the electronic factors occurred for intersystem crossing, electronic structures and energies of singlet and triplet states were calculated using the time-dependent density functional theory (TD-DFT) method at the ω B97X-D/6-31G(d,p) level. The TD-DFT is one of the theories treating for the excited states. The functional (ω B97X-D), which was different from that used previously (B3LYP/6-31G(d)),⁸³ is the long-range corrected one with dispersion effect.

Generally, it is well-known that an intersystem process is dominated by spin-orbit interactions, as rationalized by the El-Sayed rule^{64–66} and the energy gap rule.⁹⁰ Therefore, we focused on the nature and excitation energies of the lowest

Table 3. Excitation Energy, Oscillator Strength, Main Transition Orbital, and Their Contribution Calculated for Nap 1 and Nap 2 Using TD-DFT (ω B97X-D/6-31G(d,p))

entry	state	excitation energy [eV]	oscillator strength	main transition orbital	contribution			
Nap 1	T ₆	4.53	-	HOMO-5 – LUMO	0.27			
				HOMO-1 – LUMO	0.18			
				HOMO-1 – LUMO+1	0.1			
	S ₁	4.55	0.018	HOMO-2 – LUMO	0.31			
				HOMO – LUMO	0.41			
				HOMO – LUMO+1	0.23			
T ₇	4.62	-	HOMO-2 – LUMO+1	0.63				
Nap 2	T ₆	4.58	-	HOMO-2 – LUMO+1	0.42			
				HOMO-1 – LUMO+1	0.2			
				HOMO – LUMO+1	0.17			
	S ₁	4.59	0.011	HOMO-2 – LUMO	0.18			
				HOMO-1 – LUMO	0.26			
				HOMO – LUMO	0.18			
Anth 1	S ₂	4.73	0.056	HOMO – LUMO	0.74			
				T ₂	3.35	-	HOMO-5 – LUMO	0.30
				HOMO-3 – LUMO			0.22	
	HOMO – LUMO+4	0.41						
	S ₁	3.62	0.14	HOMO – LUMO	0.98			
	Anth 2	T ₃	3.71	-	HOMO-1 – LUMO	0.88		
T ₂		3.36	-	HOMO-4 – LUMO	0.42			
				HOMO – LUMO+2	0.35			
				HOMO – LUMO	1.0			
S ₁		3.63	0.13	HOMO – LUMO	0.29			
T ₃		3.74	-	HOMO-1 – LUMO	0.50			
Py 1a	T ₆	3.88	-	HOMO – LUMO+1	0.32			
				HOMO – LUMO+1	0.1			
				HOMO – LUMO+4	0.33			
	S ₁	3.96	0.42	HOMO – LUMO	0.82			
	S ₂	4.03	0.057	HOMO-1 – LUMO	0.45			
				HOMO – LUMO+1	0.45			
Py 2a				T ₇	4.12	-	HOMO-1 – LUMO+1	0.91
	T ₅	3.92	-	HOMO-5 – LUMO	0.37			
				HOMO – LUMO+3	0.4			
				HOMO-1 – LUMO	0.21			
	S ₁	4.03	0.21	HOMO – LUMO	0.52			
				HOMO – LUMO+1	0.22			
HOMO-1 – LUMO				0.25				
S ₂	4.05	0.18	HOMO – LUMO	0.41				
			HOMO – LUMO+1	0.30				
			T ₆	4.11	-	HOMO-1 – LUMO+1	0.88	

excited singlet states (S₁) and the excited triplet states around S₁ of *N*-alkyl and *N,N*-dialkyl carboxamides.

Clear *n*– π^* transition was not observed for any of the compounds at S₁ or at the excited triplet states around S₁. In other words, for the transitions that might be assigned to *n*– π^* , almost all electronic structures in the ground state had shapes similar to a mixture of *n*- and π -orbitals. These molecular orbitals are shown in Supplementary Figure 6S, and several parameters, including excitation energies and oscillator strength only for the singlet excited states, are summarized in Table 3.

From the shapes of the orbitals, it is expected that the *n*-orbital contributions would be relatively small in **Py 1a** and **Py 2a**. Therefore, the mixing between S₁ and its near triplet state can be considered to be weak, which means the intersystem

crossing would be inefficient. As a result, **Py 1a** and **Py 2a** showed high fluorescence efficiencies at 78 K.

When comparing the results with those obtained for pyrene, the anthracene derivatives also seem to possess only minor *n*-orbital contributions, e.g., HOMO-3 and HOMO-5 in **Anth 1** and HOMO-1 in **Anth 2**. However, it should be noted that the energy gap between S₁ and T₂ was 0.27 eV for both **Anth 1** and **Anth 2**, and this value was much larger than that of unsubstituted anthracene (0.05 eV).⁹³ We think that such a large energy gap is more favorable for fluorescence emission than the mixing between the *n*– π^* and π – π^* states and that, as a result, the intersystem crossing contributions were reduced in **Anth 1** and **Anth 2** and stronger emissions were observed at 78 K compared to that of anthracene.

On the other hand, the naphthalene derivatives showed relatively clear n-orbital components such as HOMO-1, HOMO-2, and HOMO-5 in **Nap 1** and HOMO-1 and HOMO-2 in **Nap 2**. In addition, the energy gaps between S_1 and the triplet around S_1 of **Nap 1** and **Nap 2** were very small. This means that the intersystem crossing processes were highly likely to occur for **Nap 1** and **Nap 2**. Furthermore, in terms of **Nap 2**, the second lowest singlet excited state, S_2 , was the closest to the upper state of S_1 . In this situation, it is possible that a “proximity effect”,^{100–102} which induced internal conversion, could have occurred. Therefore, the calculation results supported two reasons for the low fluorescence of **Nap 2**, i.e., the presence of both intersystem crossing and internal conversion. However, these could not explain the high fluorescence of **Nap 1** compared to **Nap 2**. While it is very difficult to estimate the detailed contributions of $n-\pi^*$ transitions, slight differences in either or both such contributions and the energy gap between S_1 and the triplet may be responsible for this difference in the fluorescence levels of the two molecules.

Geometries of N-Alkyl and N,N-Dialkyl Aromatic Carboxamides in Excited State. As shown in Table 4 and Figure 7S

Table 4. Relationships between Ground and First Excited Singlet States of N-Alkyl and N,N-Dialkyl Carboxamides

entry	dihedral angle (deg)		N–(C=O) bond length [Å]		$(\mu_e - \mu_g)^{2a}$
	S_0	S_1	S_0	S_1	
Nap 1	26.9	10.5	1.364	1.381	2.24
Nap 2	43.2	1.3	1.371	1.450	4.8
Anth 1	64.4	50.1	1.363	1.368	0.088
Anth 2	82.9	79.5	1.363	1.360	0.0038
Py 1a	45.4	25.6	1.363	1.381	0.044
Py 2a	76.8	1.2	1.366	1.450	14.2

^a μ_e , μ_g : Dipole moments for excited state and ground state, respectively.

(Supporting Information), the optimized structures of *N*-alkyl and *N,N*-dialkyl aromatic carboxamides in the excited states were calculated. It was found that the dihedral angles between the aromatic rings and carbonyl groups of *N*-alkyl and *N,N*-dialkyl naphthalene and pyrene carboxamides tended to be more planar in the excited states. Furthermore, the lengths of the N–(C=O) bonds were extended in the optimized states, especially in **Nap 2** and **Py 2a**. This implies that the partial double bond characteristics of the N–(C=O) bond in amide groups were decreased. Calculations indicated that the conjugations between aromatic rings and carbonyl groups were more favorable than those between amide units for the rearrangement from Franck–Condon states to optimized states. In anthracene-9-carboxylic acid or its ester derivatives, it has been demonstrated that such a planar structure prevents the internal conversion process by inducing rigidity.^{73,76–79} On the other hand, in *N,N*-dialkyl carboxamides, it is considered that the decrease in the partial double bond characteristics of the N–(C=O) bond causes molecular motions in the amine parts. In addition, it is likely that such molecular motions caused either or both the “loose bolt effect” and “free-rotor effect”,⁹⁰ known as factors that induce the internal conversion from S_1 to S_0 because of stretching σ -bond and twisted π -bond, respectively. Therefore, considering that tendencies to be planar were more strongly emphasized in *N,N*-dialkyl

carboxamides **Nap 2** and **Py 2a**, we inferred that the extremely low luminescence properties of **Nap 2** and **Py 2a** were not only because of intersystem crossing but also because of internal conversion induced by such effects. However, the above-mentioned relationships between the planarity of structures and the emission properties of anthracene derivatives did not match those of naphthalene and pyrene derivatives. This is likely because the changes in dihedral angle between the anthracene ring and carbonyl groups and bond lengths of N–(C=O) in amide groups were small and subtle in both **Anth 1** and **Anth 2**. However, it can be said with certainty that the relatively unsubstituted anthracene chromophore lost its rigidity due to the introduction of *N*-alkyl and *N,N*-dialkyl carboxamide groups. Therefore, we attributed the improved emission of **Anth 1** and **Anth 2** at 78 K to the effects induced by *N*-alkyl and *N,N*-dialkyl carboxamide groups.

Proposed Photoluminescence Mechanism. On the basis of our experiments, we can estimate the contributions from intersystem crossing and internal conversion of naphthalene, anthracene, pyrene, and their *N*-alkyl and *N,N*-dialkyl carboxamide derivatives. Considering that the fluorescence quantum yields increased in the order of naphthalene < anthracene < pyrene, it can be said that contribution from intersystem crossing increased in the reverse order. Using this sequence, objective estimations with respect to *N*-alkyl and *N,N*-dialkyl carboxamides were made and are summarized in Table 5.

Table 5. Contributions from Intersystem Crossing and Internal Conversion of N-Alkyl and N,N-Dialkyl Aromatic Carboxamides

entry	intersystem crossing ^a	internal conversion ^a
naphthalene	++++	–
Nap 1	++	+
Nap 2	++++	+++
anthracene	+++	–
Anth 1	++	++
Anth 2	++	++
pyrene	++	–
Py 1a	–	+
Py 2a	+	+++

^aNumber of (+) symbols indicate the tendency to accept the corresponding processes.

As mentioned above, the deactivation processes of naphthalene, anthracene, and pyrene involve intersystem crossing. However, in **Nap 1** and the anthracene and pyrene derivatives, internal conversion is likely to be a more competitive component. In other words, the *N*-alkyl and *N,N*-dialkyl groups serve to reduce the contributions from intersystem crossing. Therefore, we believe that the fluorescence properties of the *N*-alkyl and *N,N*-dialkyl carboxamides depend on increased contributions from internal conversion and decreased contributions from intersystem crossing. The contributions from the internal conversion of *N*-alkyl and *N,N*-dialkyl carboxamides tend to be increased when the dihedral angles between the polycyclic aromatic rings and carbonyl groups approach a planar structure in the excited states, and those from the intersystem crossing tend to depend on the nature of the chromophore itself. These insights mean that the fluorescence properties of *N*-alkyl and *N,N*-dialkylpolycyclic aromatic carboxamides may be controlled by

the choices of chromophores and amide substituents, in addition to solvent viscosity and temperature. It can be said that such photophysical characteristics are not seen in other aromatic carbonyl compounds, and these “unstable” emission properties are unique.

CONCLUSIONS

In summary, the photophysical properties and fluorescence mechanisms of *N*-alkyl and *N,N*-dialkyl polycyclic aromatic carboxamides were investigated, and the effects of the substituents on polycyclic aromatic hydrocarbon chromophores were evaluated. We chose naphthalene, anthracene, and pyrene as the polycyclic aromatic hydrocarbons and prepared a number of different target compounds. UV-vis and fluorescence spectra of the molecules in solvents with different polarities indicated that such compounds did not form charge transfer states. Investigation of the dependence of the fluorescence properties on the solvents' thermal and viscosity characteristics, along with TD-DFT calculations, showed that, in almost all the *N*-alkyl and *N,N*-dialkyl carboxamides, the contributions of intersystem crossing were reduced and those of the internal conversions were increased. These photophysical characteristics are specific and unique to aromatic carbonyl compounds. Importantly, the calculations indicated that the intersystem crossing and internal conversion contributions could be controlled by selecting the appropriate aromatic chromophore and the structure of the amide substituents, in addition to solvent viscosity and temperature. We believe that such effects are caused by the *N*-alkyl and *N,N*-dialkyl carboxamides groups, and these insights into the substitution effects will enable the successful design and development of new emission materials. In future work, we will attempt to create new functional emission dyes using this new knowledge.

EXPERIMENTAL SECTION

Synthesis of *N*-Alkyl and *N,N*-Dialkyl Polyaromatic Carboxamides. **Synthesis of *N*-Benzyl-2-naphthamide (Nap 1).** Naphthalene-2-carboxylic acid chloride (1.0 g, 5.2 mmol), triethylamine (1.5 g, 15 mmol), and CHCl_3 (20 mL) were placed in a 100-mL two-necked flask under nitrogen. Benzylamine (1.6 g, 15 mmol) was added dropwise to the above solution at 0 °C. The mixture was then allowed to be gradually warmed to rt. It was then stirred overnight. Subsequently, it was quenched with 1 N HCl to separate the formed organic layer. The organic layer was washed with brine. It was dried over MgSO_4 and then evaporated in vacuo. The residue was subjected to silica column chromatography using ethyl acetate/hexane = 1:3. Subsequent recrystallization in ethyl acetate afforded amide as a colorless solid (1.2 g, 89%). Mp 140.7–142.5 °C; ^1H NMR (400 MHz, CDCl_3) δ 8.31 (s, 1H), 7.91–7.84 (m, 4H), 7.58–7.51 (m, 2H), 7.42–7.26 (m, 5H), 6.57 (s, 1H), 4.72–4.71 (d, J = 5.67 Hz, 2H) ppm; ^{13}C NMR (100 MHz, CDCl_3) δ 167.4, 138.2, 134.7, 132.5, 131.5, 128.9, 128.7, 128.4, 127.9, 127.7, 127.6, 127.5, 127.4, 126.7, 123.6, 44.1 ppm; FT-IR (KBr) 3290, 3055, 1637, 1624, 1548, 1496, 1450, 1436, 1415, 1361, 1321, 1264, 1208, 1147, 1120, 1078, 1049, 1019 cm^{-1} . MS (FAB) calcd for $\text{C}_{18}\text{H}_{16}\text{NO}$ 262.1232, found 262.1231 ($[\text{M} + \text{H}]^+$). Anal. Calcd for $\text{C}_{18}\text{H}_{15}\text{NO}$: C, 82.73; H, 5.79; N, 5.36. Found: C, 82.85; H, 5.71; N, 5.38.

Synthesis of *N,N*-Diethyl-2-naphthamide (Nap 2). Naphthalene-2-carboxylic acid chloride (1.0 g, 5.2 mmol), triethylamine (1.5 g, 15 mmol), and CHCl_3 (20 mL) were placed in a 100-mL two-necked flask under nitrogen. Diethylamine (0.44 g, 6.0 mmol) was added dropwise to the above solution at 0 °C. The mixture was then allowed to be gradually warmed to rt. It was then stirred for 6 h. Subsequently, it was quenched with 1 N HCl to separate the formed organic layer.

The organic layer was washed with brine. It was dried over MgSO_4 and then evaporated in vacuo. The residue was subjected to silica column chromatography using ethyl acetate/hexane = 1:5. Subsequent recrystallization in ethyl acetate afforded amide as a colorless oil (1.0 g, 88%). ^1H NMR (400 MHz, CDCl_3) δ 7.88–7.84 (m, 4H), 7.54–7.46 (m, 3H), 3.60–3.31 (m, 4H), 1.28–1.13 (m, 6H) ppm; ^{13}C NMR (100 MHz, CDCl_3) δ 171.2, 134.5, 133.3, 132.7, 128.2, 128.1, 127.7, 126.6, 125.6, 123.8, 43.3, 39.2, 14.2, 12.9 ppm; FT-IR (KBr) 3054, 2972, 2943, 1627, 1480, 1454, 1424, 1381, 1363, 1348, 1314, 1288, 1243, 1218, 1176, 1130, 1088 cm^{-1} . MS (FAB) calcd for $\text{C}_{15}\text{H}_{18}\text{NO}$ 228.1388, found 228.1389 ($[\text{M} + \text{H}]^+$).

Synthesis of *N*-Benzyl-*N*-diethylantracene-9-carboxamide (Anth 1). Anthracene-9-carboxylic acid chloride (1.0 g, 4.2 mmol), triethylamine (1.2 g, 12 mmol), and CHCl_3 (20 mL) were placed in a 100-mL two-necked flask under nitrogen. Benzylamine (1.3 g, 12 mmol) was added dropwise to the above solution at 0 °C. The mixture was then allowed to be gradually warmed to rt. It was then stirred for 12 h. Subsequently, it was quenched with 1 N HCl to separate the formed organic layer. The organic layer was washed with brine. It was dried over MgSO_4 and then evaporated in vacuo. The residue was subjected to silica column chromatography using ethyl acetate/hexane = 1:3. Subsequent recrystallization in ethyl acetate afforded amide as a colorless solid (0.99 g, 76%). Mp 158.1–160.0 °C; ^1H NMR (400 MHz, CDCl_3) δ 8.46 (s, 1H), 8.08–8.06 (d, J = 8.54 Hz, 2H), 8.00–7.98 (d, J = 8.17 Hz, 2H), 7.59–7.25 (m, 9H), 4.88–4.87 (d, J = 5.61 Hz, 2H) ppm; ^{13}C NMR (100 MHz, CDCl_3) δ 169.3, 137.8, 131.5, 131.0, 128.8, 128.5, 128.3, 128.1, 128.0, 127.8, 126.7, 125.5, 125.0, 44.3 ppm; FT-IR (KBr) 3253, 3054, 1631, 1563, 1552, 1454, 1445, 1348, 1292, 1265, 1081, 1027, 1012 cm^{-1} . MS (FAB) calcd for $\text{C}_{22}\text{H}_{17}\text{NONa}$ 334.1208, found 334.1209 ($[\text{M} + \text{Na}]^+$). Anal. Calcd for $\text{C}_{22}\text{H}_{17}\text{NO}$: C, 84.86; H, 5.50; N, 4.50. Found: C, 84.86; H, 5.50; N, 4.48.

Synthesis of *N,N*-Diethylantracene-9-carboxamide (Anth 2). Anthracene-9-carboxylic acid chloride (1.0 g, 4.2 mmol), triethylamine (1.2 g, 12 mmol), and CHCl_3 (20 mL) were placed in a 100-mL two-necked flask under nitrogen. Diethylamine (0.88 g, 12 mmol) was added dropwise to the above solution at 0 °C. The mixture was then allowed to be gradually warmed to rt. It was then stirred for 12 h. Subsequently, it was quenched with 1 N HCl to separate the formed organic layer. The organic layer was washed with brine. It was dried over MgSO_4 and then evaporated in vacuo. The residue was subjected to silica column chromatography using ethyl acetate/hexane = 1:5. Subsequent recrystallization in ethyl acetate afforded amide as a colorless solid (1.1 g, 95%). Mp 116.5–118.5 °C; ^1H NMR (400 MHz, CDCl_3) δ 8.24 (s, 1H), 8.02–7.90 (m, 4H), 7.51–7.44 (m, 4H), 3.89–3.84 (dd, J = 7.13 Hz, 2H), 3.04–2.99 (dd, J = 7.01 Hz, 2H), 1.52–1.48 (t, J = 7.13 Hz, 3H), 0.87–0.83 (t, J = 7.19 Hz, 3H) ppm; ^{13}C NMR (100 MHz, CDCl_3) δ 169.4, 131.4, 131.1, 128.5, 127.4, 127.2, 126.4, 125.4, 124.8, 43.1, 38.9, 14.0, 13.1 ppm; FT-IR (KBr) 2976, 2933, 1618, 1557, 1521, 1489, 1473, 1430, 1406, 1380, 1364, 1345, 1315, 1287, 1264, 1220, 1160, 1141, 1100, 1081, 1028, 1012 cm^{-1} . MS (FAB) calcd for $\text{C}_{19}\text{H}_{19}\text{NONa}$ 300.1364, found 300.1366 ($[\text{M} + \text{Na}]^+$). Anal. Calcd for $\text{C}_{19}\text{H}_{19}\text{NO}$: C, 82.28; H, 6.90; N, 5.05. Found: C, 82.57; H, 7.13; N, 5.13.

Synthesis of *N*-Benzylpyrene-1-carboxamide (Py 1a). Pyrene-1-carboxylic acid chloride (0.54 g, 2.0 mmol), triethylamine (0.61 g, 6 mmol), and CHCl_3 (20 mL) were placed in a 100-mL two-necked flask under nitrogen. Benzylamine (0.64 g, 6.0 mmol) was added dropwise to the above solution at 0 °C. The mixture was then allowed to be gradually warmed to rt. It was then stirred overnight. Subsequently, it was quenched with 1 N HCl to separate the formed organic layer. The organic layer was washed with brine. It was dried over MgSO_4 and then evaporated in vacuo. The residue was subjected to silica column chromatography using ethyl acetate/hexane = 1:2. Subsequent recrystallization in ethyl acetate afforded amide as a colorless solid (0.64 g, 95%). Mp 160.9–162.5 °C; ^1H NMR (400 MHz, CDCl_3) δ 8.65–8.63 (d, J = 9.09 Hz, 1H), 8.25–8.04 (d, 8H), 7.49–7.47 (d, J = 7.01 Hz, 2H), 7.43–7.32 (m, 3H), 6.42 (s, 1H), 4.85–4.84 (d, J = 5.37 Hz, 2H) ppm; ^{13}C NMR (100 MHz, CDCl_3) δ 169.8, 138.3, 132.3, 131.0, 130.5, 130.5, 128.7, 128.4, 127.8, 127.5,

126.9, 126.1, 125.6, 125.5, 124.4, 124.3, 124.2, 124.1, 124.0, 44.1 ppm; FT-IR (KBr) 3274, 3030, 2919, 1631, 1531, 1291 cm^{-1} . MS (FAB) calcd for $\text{C}_{24}\text{H}_{17}\text{NONa}$ 358.1208, found 358.1208 ($[\text{M} + \text{Na}]^+$). Anal. Calcd for $\text{C}_{24}\text{H}_{17}\text{NO}$: C, 85.94; H, 5.11; N, 4.18. Found: C, 85.64; H, 4.74; N, 4.14.

Synthesis of *N-n*-Butylpyrene-1-carboxamide (Py 1b). Pyrene-1-carboxylic acid chloride (0.54 g, 2.0 mmol), triethylamine (0.61 g, 6.0 mmol), and CHCl_3 (20 mL) were placed in a 100-mL two-necked flask under nitrogen. *n*-Butylamine (0.44 g, 6.0 mmol) was added dropwise to the above solution at 0 °C. The mixture was then allowed to be gradually warmed to rt. It was then stirred overnight. Subsequently, it was quenched with 1 N HCl to separate the formed organic layer. The organic layer was washed with brine. It was dried over MgSO_4 and then evaporated in vacuo. The residue was subjected to silica column chromatography using ethyl acetate/hexane = 1:3. Subsequent recrystallization in ethyl acetate afforded amide as a colorless solid (0.43 g, 72%). Mp 159.5–161.5 °C; ^1H NMR (400 MHz, CDCl_3) δ 8.59–8.56 (d, J = 9.51 Hz, 1H), 8.24–8.03 (m, 8H), 6.10 (s, 1H), 3.67–3.62 (m, 2H), 1.76–1.69 (m, 2H), 1.47–1.56 (m, 2H), 1.04–1.01 (t, J = 7.38 Hz, 3H) ppm; ^{13}C NMR (100 MHz, CDCl_3) δ 169.9, 132.2, 131.3, 131.1, 130.6, 128.4, 128.3, 127.0, 126.2, 125.6, 125.5, 124.6, 124.4, 124.3, 124.3, 124.1, 40.0, 31.8, 20.2, 13.8 ppm; FT-IR (KBr) 3297, 3042, 2955, 2931, 2871, 1621, 1601, 1551, 1536, 1470, 1291, 1155 cm^{-1} . MS (FAB) calcd for $\text{C}_{21}\text{H}_{19}\text{NONa}$ 324.1364, found 324.1360 ($[\text{M} + \text{Na}]^+$). Anal. Calcd for $\text{C}_{21}\text{H}_{19}\text{NO}$: C, 83.69; H, 6.35; N, 4.65. Found: C, 83.63; H, 6.18; N, 4.63.

Synthesis of *N-tert*-Butylpyrene-1-carboxamide (Py 1c). Pyrene-1-carboxylic acid chloride (0.54 g, 2.0 mmol), triethylamine (0.61 g, 6.0 mmol), and CHCl_3 (20 mL) were placed in a 100-mL two-necked flask under nitrogen. *tert*-Butylamine (0.44 g, 6.0 mmol) was added dropwise to the above solution at 0 °C. The mixture was then allowed to be gradually warmed to rt. It was then stirred overnight. Subsequently, it was quenched with 1 N HCl to separate the formed organic layer. The organic layer was washed with brine. It was dried over MgSO_4 and then evaporated in vacuo. The residue was subjected to silica column chromatography using ethyl acetate/hexane = 1:3. Subsequent recrystallization in ethyl acetate afforded amide as a colorless solid (0.45 g, 74%). Mp 233.0–235.0 °C; ^1H NMR (400 MHz, CDCl_3) δ 8.55–8.53 (d, J = 8.66 Hz, 1H), 8.24–8.03 (m, 8H), 5.93 (s, 1H), 1.61 (s, 9H) ppm; ^{13}C NMR (100 MHz, CDCl_3) δ 169.5, 132.6, 132.2, 131.2, 130.7, 128.5, 128.4, 128.2, 127.1, 126.2, 125.7, 125.6, 124.7, 124.5, 124.4, 124.3, 52.3 ppm; FT-IR (KBr) 3326, 3045, 2976, 1639, 1601, 1521, 1446, 1384, 1354, 1330, 1297, 1220, 1151. cm^{-1} . MS (FAB) calcd for $\text{C}_{21}\text{H}_{19}\text{NONa}$ 324.1364, found 324.1360 ($[\text{M} + \text{Na}]^+$). Anal. Calcd for $\text{C}_{21}\text{H}_{19}\text{NO}$: C, 83.69; H, 6.35; N, 4.65. Found: C, 83.66; H, 5.99; N, 4.64.

Synthesis of *N,N*-Diethylpyrene-1-carboxamide (Py 2a). Pyrene-1-carboxylic acid chloride (1.1 g, 4.1 mmol), triethylamine (1.2 g, 12 mmol), and CHCl_3 (20 mL) were placed in a 100-mL two-necked flask under nitrogen. Diethylamine (0.88 g, 12 mmol) was added to the above solution at 0 °C. The mixture was then allowed to be gradually warmed to rt. It was then stirred overnight. Subsequently, it was quenched with 1 N HCl to separate the formed organic layer. The organic layer was washed with brine. It was dried over MgSO_4 and then evaporated in vacuo. The residue was subjected to silica column chromatography using ethyl acetate/hexane = 1:5. Subsequent recrystallization in ethyl acetate afforded amide as a colorless solid (0.70 g, 57%). Mp 108.5–109.5 °C; ^1H NMR (400 MHz, CDCl_3) δ 8.19–7.89 (m, 9H), 3.19–3.61 (m, 2H), 3.13–3.06 (m, 2H), 1.45–1.41 (t, J = 7.07 Hz, 3H), 0.95–0.92 (t, J = 7.07 Hz, 3H) ppm; ^{13}C NMR (100 MHz, CDCl_3) δ 170.6, 132.0, 131.3, 131.1, 130.8, 128.5, 127.9, 127.2, 127.1, 126.2, 125.5, 125.4, 124.6, 124.5, 124.4, 123.9, 123.3, 43.2, 39.2, 14.2, 13.1 ppm; FT-IR (KBr) 3039, 2969, 1624, 1510, 1473, 1455, 1428, 1377, 1346, 1312, 1284, 1217, 1183, 1156, 1142, 1123, 1096, 1085 cm^{-1} . MS (FAB) calcd for $\text{C}_{21}\text{H}_{19}\text{NONa}$ 324.1364, found 324.1367 ($[\text{M} + \text{Na}]^+$). Anal. Calcd for $\text{C}_{21}\text{H}_{19}\text{NO}$: C, 83.69; H, 6.35; N, 4.65. Found: C, 83.49; H, 6.29; N, 4.68.

Synthesis of Piperidin-1-yl(pyren-1-yl)methanone (Py 2b). Pyrene-1-carboxylic acid chloride (0.5 g, 1.9 mmol), triethylamine (0.6 g, 6 mmol), and CHCl_3 (20 mL) were placed in a 100-mL two-necked

flask under nitrogen. Piperidine (0.5 g, 6 mmol) was added to the above solution at 0 °C. The mixture was then allowed to be gradually warmed to rt. It was then stirred overnight. Subsequently, it was quenched with 1 N HCl to separate the formed organic layer. The organic layer was washed with brine. It was dried over MgSO_4 and then evaporated in vacuo. The residue was subjected to silica column chromatography using ethyl acetate/hexane = 1:5. Subsequent recrystallization in hexane afforded amide as a colorless solid (0.47 g, 79%). Mp 148.5–150.5 °C; ^1H NMR (400 MHz, CDCl_3) δ 8.19–7.89 (m, 9H), 4.02–3.88 (m, 2H), 3.13–3.10 (m, 2H), 1.85–1.76 (m, 2H), 1.69–1.63 (m, 2H), 1.40–1.35 (m, 2H) ppm; ^{13}C NMR (100 MHz, CDCl_3) δ 169.6, 131.6, 131.1, 130.8, 128.5, 128.0, 127.3, 127.1, 126.2, 125.6, 125.4, 124.7, 124.5, 124.0, 123.5, 48.3, 42.8, 26.6, 25.8, 24.5 ppm; FT-IR (KBr) 3039, 2988, 2939, 2857, 1620, 1508, 1464, 1428, 1367, 1348, 1285, 1270, 1201, 1181, 1141, 1126, 1087, 1024 cm^{-1} . MS (FAB) calcd for $\text{C}_{22}\text{H}_{19}\text{NO}$ 313.1467, found 313.1469 (M^+). Anal. Calcd for $\text{C}_{22}\text{H}_{19}\text{NO}$: C, 84.31; H, 6.11; N, 4.47. Found: C, 84.54; H, 6.04; N, 4.47.

Synthesis of *N-Benzyl-N-tert*-butylpyrene-1-carboxamide (Py 2c). Pyrene-1-carboxylic acid chloride (1.1 g, 4.1 mmol), triethylamine (1.2 g, 12 mmol), and CHCl_3 (20 mL) were placed in a 100-mL two-necked flask under nitrogen. *N-tert*-Butylbenzylamine (2.0 g, 12 mmol) was added dropwise to the above solution at 0 °C. The mixture was then allowed to be gradually warmed to rt. It was then stirred overnight. Subsequently, it was quenched with 1 N HCl to separate the formed organic layer. The organic layer was washed with brine. It was dried over MgSO_4 and then evaporated in vacuo. The residue was subjected to silica column chromatography using ethyl acetate/hexane = 1:5. Subsequent recrystallization in ethyl acetate afforded amide as a colorless solid (0.82 g, 51%). Mp 213.5–214.7 °C; ^1H NMR (400 MHz, CDCl_3) δ 8.21–7.94 (m, 9H), 7.26–7.14 (m, 5H), 4.52–4.50 (d, J = 6.52 Hz, 2H), 1.69 (s, 9H) ppm; ^{13}C NMR (100 MHz, CDCl_3) δ 173.0, 139.6, 133.7, 131.2, 131.2, 130.8, 128.7, 128.4, 127.8, 127.2, 126.9, 126.9, 126.2, 126.0, 125.6, 125.4, 124.7, 124.6, 124.6, 123.7, 123.4, 58.7, 51.6, 29.0 ppm; FT-IR (KBr) 2956, 1626, 1507, 1495, 1454, 1395, 1358, 1276, 1255, 1195, 1176, 1159, 1144, 1132, 1076, 1026 cm^{-1} . MS (EI) calcd for $\text{C}_{28}\text{H}_{25}\text{NO}$ 391.1936, found 391.1938 (M^+). Anal. Calcd for $\text{C}_{28}\text{H}_{25}\text{NO}$: C, 85.90; H, 6.44; N, 3.58. Found: C, 85.67; H, 6.52; N, 3.59.

Synthesis of *N-tert*-Butyl-*N*-ethylpyrene-1-carboxamide (Py 2d). Pyrene-1-carboxylic acid chloride (1.1 g, 4.1 mmol), triethylamine (1.2 g, 12 mmol), and CHCl_3 (20 mL) were placed in a 100-mL two-necked flask under nitrogen. *N-tert*-Butylethylamine (1.2 g, 12 mmol) was added to the above solution at 0 °C. The mixture was then allowed to be gradually warmed to rt. It was then stirred overnight. Subsequently, it was quenched with 1 N HCl to separate the formed organic layer. The organic layer was washed with brine. It was dried over MgSO_4 and then evaporated in vacuo. The residue was subjected to silica column chromatography using ethyl acetate/hexane = 1:5. Subsequent recrystallization in hexane afforded amide as a colorless solid (0.58 g, 43%). Mp 118.5–120.5 °C; ^1H NMR (400 MHz, CDCl_3) δ 8.21–7.91 (m, 9H), 3.38–3.15 (m, 2H), 1.74 (s, 9H), 0.98–0.94 (t, J = 7.38 Hz, 3H) ppm; ^{13}C NMR (100 MHz, CDCl_3) δ 172.0, 134.4, 131.1, 130.9, 130.8, 128.3, 127.6, 127.1, 126.7, 126.1, 125.4, 125.2, 124.6, 124.5, 123.9, 123.3, 57.4, 41.8, 29.0, 17.4 ppm. FT-IR (KBr) 3041, 2958, 1624, 1510, 1489, 1454, 1397, 1379, 1360, 1281, 1211, 1179, 1146, 1113, 1079, 1040 cm^{-1} . MS (FAB) calcd for $\text{C}_{23}\text{H}_{23}\text{NO}$ 329.1780, found 329.1779 (M^+).

■ ASSOCIATED CONTENT

● Supporting Information

Additional experimental methods for polycyclic aromatic hydrocarbons with *N*-alkyl or *N,N*-dialkyl carboxamide groups. The results of calculations (Figure S1, Figure S6–S7) and solvent dependence (Figure S2–S5, Table S1–S3), synthesis conditions and ^1H NMR and ^{13}C NMR spectra (Figure S8–S13). This material is available free of charge via the Internet at <http://pubs.acs.org>.

AUTHOR INFORMATION

Corresponding Author

*E-mail: konishi.g.aa@m.titech.ac.jp.

Notes

The authors declare no competing financial interest.

ACKNOWLEDGMENTS

We thank Prof. Katsumi Tokumaru (Emeritus Professor of Tsukuba University) for helpful discussion.

REFERENCES

- (1) Kumar, L.; Dhawan, S. K.; Kamalasanan, M. N.; Chandra, S. *Thin Solid Films* **2003**, *441*, 243–247.
- (2) Rajamalli, P.; Prasad, E. *Org. Lett.* **2011**, *13*, 3714–3717.
- (3) Huang, H.; Fu, Q.; Zhuang, S.; Liu, Y.; Wang, L.; Chen, J.; Ma, D.; Yang, C. *J. Phys. Chem. C* **2011**, *115*, 4872–4878.
- (4) Ihmels, H.; Meiswinkel, A.; Mohrschladt, C. J.; Otto, D.; Waidelich, M.; Towler, M.; White, R.; Albrecht, M.; Schnurpfeil, A. *J. Org. Chem.* **2005**, *70*, 3929–3938.
- (5) Park, H.; Lee, J.; Kang, I.; Chu, H. Y.; Lee, J. I.; Kwon, S. K.; Kim, Y. H. *J. Mater. Chem.* **2012**, *22*, 2695–2700.
- (6) Lyu, Y. Y.; Kwak, J.; Kwon, O.; Lee, S. H.; Kim, D.; Lee, C.; Char, K. *Adv. Mater.* **2008**, *20*, 2720–2729.
- (7) Figueira-Duarte, T. M.; Müllen, K. *Chem. Rev.* **2011**, *111*, 7260–7314.
- (8) Goel, A.; Kumar, V.; Nag, P.; Bajpai, V.; Kumar, B.; Singh, C.; Prakash, S.; Anand, R. S. *J. Org. Chem.* **2011**, *76*, 7474–7481.
- (9) Lewis, F. D.; Zhang, Y. F.; Letsinger, R. L. *J. Org. Chem.* **1997**, *62*, 8565–8568.
- (10) Seela, F.; Ingale, S. A. *J. Org. Chem.* **2010**, *75*, 284–295.
- (11) Lee, Y. H.; Lee, M. H.; Zhang, J. F.; Kim, J. S. *J. Org. Chem.* **2010**, *75*, 7159–7165.
- (12) Natarajan, B.; Gupta, S.; Ramamurthy, V.; Jayaraman, N. *J. Org. Chem.* **2011**, *76*, 4018–4026.
- (13) Sau, S. P.; Hrdlicka, P. J. *J. Org. Chem.* **2012**, *77*, 5–16.
- (14) Fujimoto, K.; Shimizu, H.; Inouye, M. *J. Org. Chem.* **2004**, *69*, 3271–3275.
- (15) Watanabe, Y.; Uchimura, M.; Araoka, F.; Konishi, G.; Watanabe, J.; Takezoe, H. *Appl. Phys. Express* **2009**, *2*, 102501.
- (16) Uchimura, M.; Watanabe, Y.; Araoka, F.; Watanabe, W.; Takezoe, H.; Konishi, G. *Adv. Mater.* **2010**, *22*, 4473–4478.
- (17) Shimizu, H.; Fujimoto, K.; Furusyo, M.; Maeda, H.; Nanai, Y.; Mizuno, K.; Inouye, M. *J. Org. Chem.* **2007**, *72*, 1530–1533.
- (18) Saito, Y.; Shinohara, Y.; Ishioroshi, S.; Suzuki, A.; Tanaka, M.; Saito, I. *Tetrahedron Lett.* **2011**, *52*, 2359–2361.
- (19) Fujimoto, K.; Yamada, S.; Inouye, M. *Chem. Commun.* **2009**, 7164–7166.
- (20) Pei, Q.; Yang, Y. *J. Am. Chem. Soc.* **1996**, *118*, 7416–7417.
- (21) Leclerc, M. *J. Polym. Sci., Part A: Polym. Chem.* **2001**, *39*, 2867–2873.
- (22) Wong, K. T.; Chien, Y. Y.; Chen, R. T.; Wang, C. F.; Lin, Y. T.; Chiang, H. H.; Hsieh, P. Y.; Wu, C. C.; Chou, C. H.; Su, Y. O.; Lee, G. H.; Peng, S. M. *J. Am. Chem. Soc.* **2002**, *124*, 11576–11577.
- (23) Mikroyannidis, J.; Fenenko, L.; Yahiro, M.; Adachi, C. *J. Polym. Sci., Part A: Polym. Chem.* **2007**, *45*, 4661–4670.
- (24) Zheng, C. J.; Zhao, W. M.; Wang, Z. Q.; Huang, D.; Ye, D.; Ou, X. M.; Zhang, X. H.; Lee, C. S.; Lee, S. T. *J. Mater. Chem.* **2010**, *20*, 1560–1566.
- (25) Kotaka, H.; Konishi, G.; Mizuno, K. *Tetrahedron Lett.* **2010**, *51*, 181–184.
- (26) Pan, J.; Zhu, W.; Lia, S.; Zeng, W.; Cao, Y.; Tian, H. *Polymer* **2005**, *46*, 7658–7669.
- (27) Zhan, X.; Tan, Z.; Domercq, B.; An, Z.; Zhang, X.; Barlow, S.; Li, Y.; Zhu, D.; Kippelen, B.; Marder, S. R. *J. Am. Chem. Soc.* **2007**, *129*, 7246–7247.
- (28) Addicott, C.; Oesterling, I.; Yamamoto, T.; Müllen, K.; Stang, P. *J. Org. Chem.* **2005**, *70*, 797–801.
- (29) Armit, D. J.; Crisp, G. T. *J. Org. Chem.* **2006**, *71*, 3417–3422.
- (30) Zhao, Z.; Xu, X.; Jiang, Z.; Lu, P.; Yu, G.; Liu, Y. *J. Org. Chem.* **2007**, *72*, 8345–8353.
- (31) Maeda, H.; Maeda, T.; Mizuno, K.; Fujimoto, K.; Shimizu, H.; Inouye, M. *Chem.—Eur. J.* **2006**, *12*, 824–831.
- (32) Gano, J. E.; Osborn, D. J.; Kodali, N.; Sekher, P.; Liu, M.; Luzik, E. D., Jr. *J. Org. Chem.* **2003**, *68*, 3710–3713.
- (33) Wang, J. L.; Zhou, Z.; Li, Y.; Pei, J. *J. Org. Chem.* **2009**, *74*, 7449–7456.
- (34) Landis, C. A.; Parkin, S. R.; Anthony, J. E. *Jpn. J. Appl. Phys.* **2005**, *44*, 39210–3922.
- (35) Maeda, H.; Inoue, Y.; Ishida, H.; Mizuno, K. *Chem. Lett.* **2001**, 1224–1225.
- (36) Asai, K.; Konishi, G.; Sumi, K.; Mizuno, K. *J. Organomet. Chem.* **2011**, *696*, 1236–1243.
- (37) Asai, K.; Konishi, G.; Sumi, K.; Mizuno, K. *J. Organomet. Chem.* **2011**, *696*, 1266–1271.
- (38) Parusel, A. B. J.; Nowak, W.; Grimme, S.; Köhler, G. *J. Phys. Chem. A* **1998**, *102*, 7149–7156.
- (39) Jung, S. O.; Yuan, W.; Ju, J. U.; Zhang, S.; Kim, Y. H.; Je, J. T.; Kwon, S. K. *Mol. Cryst. Liq. Cryst.* **2009**, *514*, 375–384.
- (40) Langhals, H.; Kinzel, S. *J. Org. Chem.* **2010**, *75*, 7781–7784.
- (41) Beinhoff, M.; Weigel, M.; Rettig, W.; Bruedgam, I.; Hartl, H.; Schlueter, A. D. *J. Org. Chem.* **2005**, *70*, 6583–6591.
- (42) Wee, K. R.; Ahn, H. C.; Son, H. J.; Han, W. S.; Kim, J. E.; Cho, D. W.; Kang, S. O. *J. Org. Chem.* **2009**, *74*, 8472–8475.
- (43) Zhao, Z.; Xu, X.; Wang, H.; Lu, P.; Yu, G.; Liu, Y. *J. Org. Chem.* **2008**, *73*, 594–602.
- (44) Chao, C. C.; Leung, M. K.; Su, Y. O.; Chiu, K. Y.; Lin, T. H.; Shieh, S. J.; Lin, S. C. *J. Org. Chem.* **2005**, *70*, 4323–4331.
- (45) Asai, K.; Konishi, G.; Sumi, K.; Kawachi, S. *Polym. Chem.* **2010**, *1*, 321–325.
- (46) Liaw, D. J.; Wang, K. L.; Chang, F. C. *Macromolecules* **2007**, *40*, 3568–3574.
- (47) Lian, W. R.; Wu, H. Y.; Wang, K. L.; Liaw, D. J.; Lee, K. R.; Lai, J. Y. *J. Polym. Sci., Part A: Polym. Chem.* **2011**, *49*, 3673–3680.
- (48) Lian, W. R.; Ho, C.; Huang, Y. C.; Liao, Y. A.; Wang, K. L.; Liaw, D. J.; Lee, K. R.; Lai, J. Y. *J. Polym. Sci., Part A: Polym. Chem.* **2011**, *49*, 5350–5357.
- (49) Lian, W. R.; Liao, Y. A.; Li, L. J.; Su, C. Y.; Liaw, D. J.; Lee, K. R.; Lai, J. Y. *Macromolecules* **2011**, *44*, 9550–9555.
- (50) Fujioka, T.; Taketani, S.; Nagasaki, T.; Matsumoto, A. *Bioconjugate Chem.* **2009**, *20*, 1879–1887.
- (51) Sagari, T. P. I.; Spehr, T.; Siebert, A.; Fuhmann-Lieker, T.; Salbeck, J. *Chem. Rev.* **2007**, *107*, 1011–1065.
- (52) Cocherel, N.; Poriel, C.; Vignau, L.; Bergamini, J.; Rault-Berthelot, J. *Org. Lett.* **2010**, *12*, 452–455.
- (53) Thirion, D.; Poriel, C.; Barriere, F.; Metivier, R.; Jeannin, O.; Rault-Berthelot, J. *J. Org. Lett.* **2009**, *11*, 4794–4797.
- (54) Luo, J.; Zhou, Y.; Niu, Z. Q.; Zhou, Q. F.; Ma, Y.; Pei, J. *J. Am. Chem. Soc.* **2007**, *129*, 13414–13415.
- (55) Sumi, K.; Konishi, G. *Molecules* **2010**, *15*, 7582–7592.
- (56) Yamaguchi, Y.; Tanaka, T.; Kobayashi, S.; Wakamiya, T.; Matsubara, Y.; Yoshida, Z. *J. Am. Chem. Soc.* **2005**, *127*, 9332–9333.
- (57) Yamaguchi, Y.; Ochi, T.; Wakamiya, T.; Matsubara, Y.; Yoshida, Z. *Org. Lett.* **2006**, *8*, 717–720.
- (58) Yamaguchi, Y.; Matsubara, Y.; Ochi, T.; Wakamiya, T.; Yoshida, Z. *J. Am. Chem. Soc.* **2008**, *130*, 13867–13869.
- (59) Kanibolotsky, A. L.; Berridge, R.; Skabara, P. J.; Perepichka, I. F.; Bradley, D. D. C.; Koeberg, M. *J. Am. Chem. Soc.* **2004**, *126*, 13695–13702.
- (60) Boldridge, D. W.; Justus, B. L.; Scott, G. W. *J. Chem. Phys.* **1984**, *80*, 3179–3184.
- (61) Hirayama, S.; Kobayashi, T. *Chem. Phys. Lett.* **1977**, *52*, 55–58.
- (62) Hirayama, S. *J. Chem. Soc. Faraday Trans. I* **1982**, *78*, 2411–2421.
- (63) Kumar, C. V.; Chattopadhyay, S. K.; Das, P. K. *Photochem. Photobiol.* **1983**, *38*, 141–152.
- (64) Lower, S. K.; El-Sayed, M. A. *Chem. Rev.* **1966**, *66*, 199–241.

- (65) Baba, M. *J. Phys. Chem. A* **2011**, *115*, 9514–9519.
- (66) Herkstroeter, W. G.; Lamola, A. A.; Hammond, G. S. *J. Am. Chem. Soc.* **1964**, *86*, 4537–4540.
- (67) Azumaya, I.; Kagechika, H.; Fujiwara, Y.; Itoh, M.; Yamaguchi, K.; Shudo, K. *J. Am. Chem. Soc.* **1991**, *113*, 2833–2838.
- (68) Lewis, F. D.; Long, T. M. *J. Phys. Chem. A* **1998**, *102*, 5327–5332.
- (69) Heldt, J. *J. Photochem. Photobiol. A Chem.* **1991**, *60*, 183–191.
- (70) Morozumi, T.; Anada, T.; Nakamura, H. *J. Phys. Chem. B* **2001**, *105*, 2923–2931.
- (71) Watkin, A. R. *J. Chem. Soc., Faraday Trans. I* **1972**, *68*, 28–36.
- (72) Underberg, W. J. M.; Schulman, S. G. *Anal. Chim. Acta* **1979**, *105*, 311–317.
- (73) Werner, T. C.; Hercules, D. M. *J. Phys. Chem.* **1969**, *73*, 2005–2011.
- (74) Tulock, J. J.; Blanchard, G. J. *J. Phys. Chem. B* **1998**, *102*, 7148–7155.
- (75) Nucci, N. V.; Zelent, B.; Vanderkooi, J. M. *J. Fluoresc.* **2007**, *18*, 41–49.
- (76) Costta, S. M. B.; Macanita, A. L.; Prieto, M. J. *J. Photochem.* **1979**, *11*, 109–119.
- (77) Werner, T. C.; Hercules, D. M. *J. Phys. Chem.* **1969**, *73*, 2005–2011.
- (78) Werner, T. C.; Hoffman, R. M. *J. Phys. Chem.* **1973**, *77*, 1611–1615.
- (79) Werner, T. C.; Lyon, D. B. *J. Phys. Chem.* **1982**, *86*, 933–939.
- (80) Okamoto, A.; Ichiba, T.; Saito, I. *J. Am. Chem. Soc.* **2004**, *126*, 8364–8366.
- (81) Yao, C.; Kraatz, H.-B.; Steer, R. P. *Photochem. Photobiol. Sci.* **2005**, *4*, 191–199.
- (82) Siegmund, K.; Daublain, P.; Wang, Q.; Trifonov, A.; Fiebig, T.; Lewis, F. D. *J. Phys. Chem. B* **2009**, *113*, 16276–16284.
- (83) Niko, Y.; Kawauchi, S.; Konishi, G. *Tetrahedron Lett.* **2011**, *52*, 4843–4847.
- (84) Niko, Y.; Konishi, G. *Macromolecules* **2012**, *45*, 2327–2337.
- (85) Werner, T. C.; Rodger, J. J. *Photochem.* **1986**, *32*, 59–68.
- (86) Sturgeon, R. C. J.; Schulman, S. G. *J. Pharm. Sci.* **1976**, *65*, 1833–1835.
- (87) Adachi, C.; Baldo, M. A.; Thompson, M. E.; Forrest, S. R. *J. Appl. Phys.* **2001**, *90*, 5048–5051.
- (88) Endo, A.; Ogasawara, M.; Takahashi, A.; Yokoyama, D.; Kato, Y.; Adachi, C. *Adv. Mater.* **2009**, *21*, 4802–4806.
- (89) Hong, Y.; Lama, J. W. Y.; Tang, B. Z. *Chem. Commun.* **2009**, 4332–4353.
- (90) Turro, N. J.; Ramamurthyl, V.; Scaiano, J. C. *Modern Molecular Photochemistry of Organic Molecules*; University Science Books: South Orange, NJ, 2010; pp288–291.
- (91) Montalti, M.; Credi, A.; Prodi, L.; Gandolfi, M. T. *Handbook of Photochemistry*, 3rd ed.; CRC Press: Boca Raton, 2006.
- (92) Yamaguchi, Y.; Matsubara, Y.; Ochi, T.; Wakamiya, T.; Yoshida, Z. *J. Am. Chem. Soc.* **2008**, *130*, 13867–13869.
- (93) Katoh, R.; Suzuki, K.; Furube, A.; Kotani, M.; Tokumaru, K. *J. Phys. Chem. C* **2009**, *113*, 2961–2965.
- (94) In this work, lifetimes and quantum yields of naphthalene, anthracene, and pyrene were measured by ourselves. This is because such photophysical parameters of classical chromophores, especially for naphthalene and pyrene, change greatly with literatures as can be seen in refs 56 and 90.
- (95) Lippert, E. *Z. Elektrochem* **1957**, *61*, 962–975.
- (96) Azumaya, I.; Yamaguchi, K.; Kagechika, H.; Saito, S.; Itai, A.; Shudo, K. *Yakugaku Zasshi* **1994**, *112*, 414–430.
- (97) Okamoto, I.; Kagechika, H.; Tanatani, A. *J. Syn. Org. Chem. Jpn.* **2000**, *58*, 14–25.
- (98) Kummer, A. D.; Kompa, C.; Niwa, H.; Hirano, T.; Kojima, S.; Michel-Beyerle, M. E. *J. Phys. Chem. B* **2002**, *106*, 7554–7559.
- (99) Matsumoto, T.; Sato, M.; Hirayama, S. *Chem. Phys. Lett.* **1971**, *13*, 13–15.
- (100) Wassam, W. A.; Lim, E. C. *J. Chem. Phys.* **1978**, *68*, 433–454.
- (101) Wassam, W. A.; Lim, E. C. *J. Chem. Phys.* **1978**, *69*, 2176–2180.
- (102) Wassam, W. A.; Lim, E. C. *J. Mol. Struct.* **1978**, *47*, 129–198.
- (103) This reference is cited in Supporting Information. Chang, Y.-H.; Hsu, M.-H.; Wang, S.-H.; Hung, L.-J.; Qian, K.; Morris-Natschke, S. L.; Hamel, E.; Kuo, S.-C.; Lee, K.-H. *J. Med. Chem.* **2009**, *52*, 4883–4891.